Green Chemistry

PAPER

View Article Online
View Journal | View Issue

Cite this: *Green Chem.*, 2021, **23**, 920

Pd-Catalysed carbonylative Suzuki–Miyaura cross-couplings using $Fe(CO)_5$ under mild conditions: generation of a highly active, recyclable and scalable 'Pd–Fe' nanocatalyst†

Zhuangli Zhu,[a,b] Zhenhua Wang,[a] Yajun Jian,[a] Huaming Sun,[a] Guofang Zhang,[a] Jason M. Lynam,[c] C. Robert McElroy,[c] Thomas J. Burden,[c] Rebecca L. Inight,[c] Ian J. S. Fairlamb,*[c] Weiqiang Zhang*[a] and Ziwei Gao*[a]

Received 7th September 2020,
Accepted 23rd November 2020

DOI: 10.1039/d0gc03036h

rsc.li/greenchem

The dual function and role of iron(0) pentacarbonyl [$Fe(CO)_5$] has been identified in gaseous CO-free carbonylative Suzuki–Miyaura cross-couplings, in which $Fe(CO)_5$ supplied CO *in situ*, leading to the propagation of catalytically active Pd–Fe nanoparticles. Compared with typical carbonylative reaction conditions, CO gas (at high pressures), specialised exogenous ligands and inert reaction conditions were avoided. Our developed reaction conditions are mild, do not require specialised CO high pressure equipment, and exhibit wide functional group tolerance, giving a library of biaryl ketones in good yields.

Introduction

Pd-Catalysed three-component coupling reactions of aryl boronic acids, carbon monoxide (CO) and aryl halides/pseudohalides, generally known as carbonylative Suzuki–Miyaura cross-coupling (*C*-SMCC) reactions,[1] display numerous synthetic advantages, particularly the ready availability of commercially available starting materials, which are typically thermally-, air- and water-stable. The *C*-SMCC reactions exhibit wide functional group compatibility, accompanied by broad substrate scope.[2] Typically, the reaction represents a straightforward and convenient process allowing access to a myriad of symmetrical and unsymmetrical biaryl ketones,[3] which are omnipresent in natural products and other synthetic target compounds, with some exhibiting favourable bioactivity and material properties.[4]

Over the last few decades we have seen practical advances in *C*-SMCCs, especially enabled through the design of new Pd (pre)catalysts.[5] However, the toxic and flammable CO gas potentially hinders wider adoption of *C*-SMCCs, especially so in academic laboratories, for which expertise and specialised equipment might be limited, with health and safety concerns being at the forefront of any decision-making process. It is also known that the CO-insertion efficiency is reduced when employing electron-deficient aryl halides,[6] which can typically be overcome by the adoption of an expensive exogenous ligand or high pressure in CO (Fig. 1a).[7]

Moving the field forward, the development of a carbonylation procedure employing the *in situ* generation of CO, as a substitute for gaseous CO, is appealing and arguably necessary

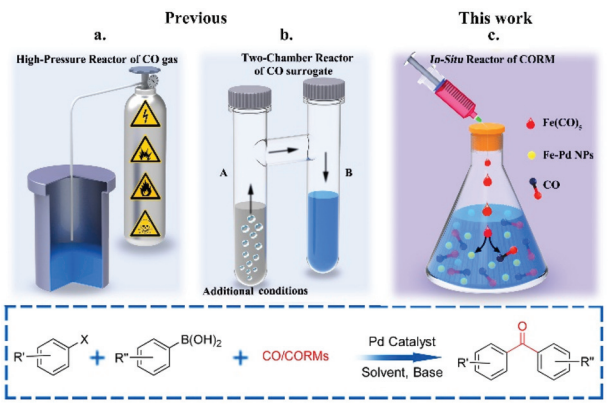

Fig. 1 Pd-Catalysed carbonylative-Suzuki–Miyaura cross-couplings (*C*-SMCC)@ (a) historical and industrially relevant carbonylative high pressure system; (b) two-chamber, with independent generation of CO; and (c) *in situ* generation of CO from a metal-based CO–RM, the metal fragment capable of modifying catalytic efficacy.

[a]*Key Laboratory of Applied Surface and Colloid Chemistry, Ministry of Education, School of Chemistry & Chemical Engineering, Shaanxi Normal University, 199 South Chang'an Road, Xi'an, China. E-mail: zwq@snnu.edu.cn, zwgao@snnu.edu.cn*
[b]*Tianjin Normal University, 393 West Binshui Road, Tianjin, China*
[c]*Department of Chemistry, University of York, Heslington, York, North Yorkshire, YO10 5DD, UK. E-mail: ian.fairlamb@york.ac.uk*
† Electronic supplementary information (ESI) available: Experimental details and characterization. See DOI: 10.1039/d0gc03036h

for general synthetic chemistry laboratories. With this point in mind several research teams have replaced CO gas with safer sources of molecular CO, *i.e.* in the form of CO-surrogates.[8,9] Indeed, leaders in the field are Skrydstrup[10] *et al.*, who have developed Pd-catalysed carbonylation reactions using *ex situ* CO generated from CO-surrogates and a specially designed two-chamber reactor (Fig. 1b). Several CO surrogates have been employed, *e.g.* 9-methyl-9*H*-fluorene-9-carbonyl chloride (COgen), silacarboxylic acids (SilaCOgen), alcohols, carbon dioxide, metal carbonyls and formic acid. These CO-surrogates degrade in a controllable manner, by different mechanisms, supplying CO gas for Pd-catalysed carbonylation reactions.[10,11]

With synthetic verstaility in mind, the well-controlled *in situ* generation of CO is essential for the development of a safe and convenient one-pot *C*-SMCC methodology. Transition metal carbonyls (TMCs) have been utilised as CO releasing molecules (CO-RMs) for therapeutic delivery of CO in biological systems,[12] a field which we have contributed to independently, and for which much is now known about CO-release rates in different media. Many readily available homoleptic TMCs are attractive CO-RMs, since many carbonyls per CO-RM can in principle be delivered in solution. More importantly, the cleavage of the M–CO bond of TMCs can be controlled by the variation of temperature. $Ni(CO)_4$ has been employed in the aminocarbonylation of vinyl halides[13*a*] and carbonylative olefination of aryl halides.[13*b*] Larhed *et al.*[14] pioneered Pd-catalysed carbonylation of O, N nucleophiles using $Cr(CO)_6$ and $Mo(CO)_6$. The solid CO-RMs were activated by microwave heating, and CO was generated *in situ* for carbonylation. Later, other solid TMCs were evaluated as CO-RMs for transition metal-catalysed organic transformations.[10] In all cases, the metal is thought to be a waste element within the reaction. Indeed, a limitation identified was that the low valence transition metal residue could poison the active Pd catalyst species, with reactions being sluggish, leading to poor yields of the carbonylative products,[15*a*] a potential issue for more challenging substrates.[15*b*,*c*] Maes *et al.* have developed methodologies employing isocyanides as CO-surrogates in Pd-catalysed cross-couplings, offering an alternative approach.[16]

In light of highly effective and catalytically competent Pd/Fe nanoparticles being discovered for C–C cross-coupling reactions,[17] we recognised that iron carbonyls could potentially play the role of CO–RMs, while modifying the properties and catalytic activity of the Pd catalyst through beneficial interactions with Fe, *i.e.* where the CO ligands are utilised for the carbonylation process and the waste Fe (oxidised) creating a more efficient Pd–Fe catalytic system *in situ*. Due to the low-price and earth abundance of iron, we envisaged that an economical, safer and environmentally friendly Pd-catalysed *C*-SMCC methodology using $Fe(CO)_5$ could be developed.

Herein, we report a benign *C*-SMCC reaction methodology, which does not require the use of CO gas or exogenous specialised ligands, where $Fe(CO)_5$ provides CO for the reaction, generating well-defined, stable and catalytically competent Fe/Pd nanoparticles *in situ*, which can be further recycled in multiple reaction runs (Fig. 1c).

Results and discussion

The *C*-SMCC of *p*-iodo-acetophenone **1a** with phenylboronic acid **2a** to give **3a** was chosen as the benchmark reaction to evaluate the viability of $Fe(CO)_5$ as a CO source and Pd catalyst modifier. A reaction pathway to the non-carbonylative Suzuki–Miyaura cross-coupled product **3a′** is competitive; thus it is critical to identify reaction conditions enabling high selectivity for **3a**. The reaction parameters, including (pre)catalysts, solvents and bases, were screened to establish the best system for the gaseous CO-free *C*-SMCC methodology (Table 1). Interestingly, without a phosphine ligand, all Pd precursors, $Pd(OAc)_2$ {note: $Pd_3(OAc)_6$}, $Pd_2(dba)_3$ (dba = 1,4-dibenzylidene acetone), $Pd(acac)_2$ (acac = acetylacetonate) and polymeric $PdCl_2$, exhibited high conversion and selectivity (entries 1–5), using as little as 0.5 mol% Pd (pre)catalyst loading (entry 2). The presence of phosphine ligands suppressed the carbonylation product **3a** yield (entries 6–12). Poor product selectivity shows that the phosphine ligands are able to facilitate the oxidative addition of **1a** to the *in situ* generated "L–Pd^0" species, but slow down the subsequent CO insertion into the Pd–C bond. We also recognise that the phosphine ligands could

Table 1 Optimization and effects of the reaction parameters[a]

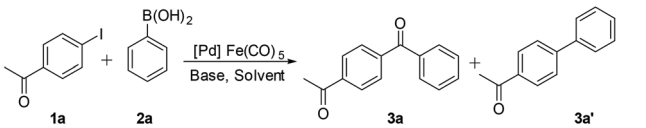

Entry	Catalyst	Ligand / Solvent/base	3a %[b]	3a'
Effect of catalyst and ligand (1 : 1)				
1	$Pd(OAc)_2$		90	7
2	$Pd(OAc)_2$[c]		86	8
3	$Pd_2(dba)_3$		80	7
4	$Pd(acac)_2$		89	7
5	$PdCl_2$		80	18
6	$PdCl_2(PPh_3)_2$		5	94
7	$Pd(OAc)_2$	PPh_3	64	31
8	$Pd(OAc)_2$	CyJohnPhos	31	22
9	$Pd(OAc)_2$	PCy_3	71	21
10	$Pd(OAc)_2$	Dppf	70	25
11	$Pd(OAc)_2$	Xphos	40	12
12	$Pd(OAc)_2$	Xantphos	48	14
Effect of solvent (3 mL) and base (2 eq.)				
13	$Pd(OAc)_2$	Toluene/K_2CO_3	87	11
14	$Pd(OAc)_2$	Dioxane/K_2CO_3	60	7
15	$Pd(OAc)_2$	Anisole/K_3PO_4	83	10
16	$Pd(OAc)_2$	Anisole/DIPEA	51	1

[a] Reaction conditions: **1a** (0.434 mmol), **2a** (1.75 eq.), $Fe(CO)_5$ (0.15 mmol), and [Pd] (1 mol%, unless otherwise stated), 80 °C, 12 h. Entries 1–12: anisole and K_2CO_3 were used. [b] Detected by ^1H NMR and confirmed by purification by silica gel chromatography. [c] $Pd_3(OAc)_6$, referred to as $Pd(OAc)_2$, (0.5 mol% in Pd).

influence Pd catalyst speciation, negatively in terms of the carbonylation selectivity in this system.

The effects of the solvent and base were further examined. It was found that the *C*-SMCC reaction proceeded well in relatively less polar solvents, such as anisole and toluene. The inorganic bases, K_2CO_3 and K_3PO_4, exhibited high substrate conversion and superior selectivity when compared against the organic base, DIPEA (entries 13–16). Other TMCs were also assessed as CORMs. Indeed, the ferrous-system performed considerably better than $Mo(CO)_6$ and $Cr(CO)_6$ (Table S2, see the ESI†). It is of particular note that using gaseous CO (balloon pressure) in place of $Fe(CO)_5$ failed to effect a successful *C*-SMCC reaction, with only the SMCC biaryl product **3a′** being formed. The outcome demonstrates that $Fe(CO)_5$ not only acts as a CO source, but also functions positively *vide infra* to enhance this specific Pd-catalysed *C*-SMCC reaction in some way.

With the optimised reaction conditions in hand {0.15 mmol $Fe(CO)_5$, 1 mol% $Pd(OAc)_2$, anisole and K_2CO_3}, various functional biaryl ketones were synthesized using the new *C*-SMCC reaction differentiated by changes in aryl substituents, either electron-donating or electron-withdrawing, of aryl iodides (Table 2) and those of phenylboronic acids (Table 3), to evaluate the scope and limitations of the new *C*-SMCC methodology.

Table 2 shows the effects of substituents in the reactions of aryl iodides. Under the best identified reaction conditions, the *para*-halogenated (Cl, Br, and F) aryl iodides gave diaryl ketones in good yields (*p*-F, **3b**, 79%, *p*-Cl, **3f**, 73%, and *p*-Br, **3n**, 74%). However, *ortho*-Cl and Br substituents led to only modest yields of cross-coupled products with 50% (**3j**) and 30% (**3o**) biaryl ketone products being generated respectively. We tentatively attribute the lowering of the yield to steric effects, which retard the oxidation addition step.[18] The presence of a methyl group at *para*-, *meta*- and *ortho*-positions led to good product yields (*p*-Me, **3c**, 84%, *m*-Me, **3g**, 74%, and *o*-Me, **3k**, 72%). The corresponding biaryl ketone products possessing methoxy groups at *para*-, *meta*- and *ortho*-positions were isolated in good yields, with 74% for **3e**, 53% for **3i** and 78% for **3m**, respectively. Meanwhile, as the length of the alkyl chain was increased to ethyl a 66% yield of **3d** was recorded. As for electron-withdrawing substituents, similar trends were noted. For example, the weakly electron-withdrawing ester group, *p*-CO_2Me, gave a good yield of 80% (**3q**), with the *p*-CO_2Et group giving a 73% yield of **3u**. In addition, the stronger electron-withdrawing substituents only lower the yields marginally (*p*-CF_3, **3h**, 57%, *p*-NO_2, **3p**, 68%, and *m*-NO_2, **3t**, 65%). We further succeeded in synthesizing the biaryl ketones containing naphthalene (**3r**, 55%) and thiophene (**3s**, 54%), which are key intermediates to interesting luminescent materials.[19]

Table 2 Pd catalyzed carbonylative Suzuki coupling reaction

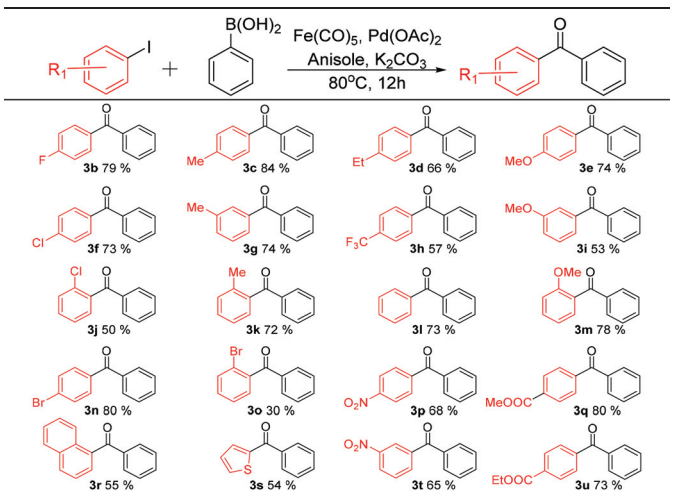

Table 3 Synthesis of biaryl ketones *via* different arylboronic acids

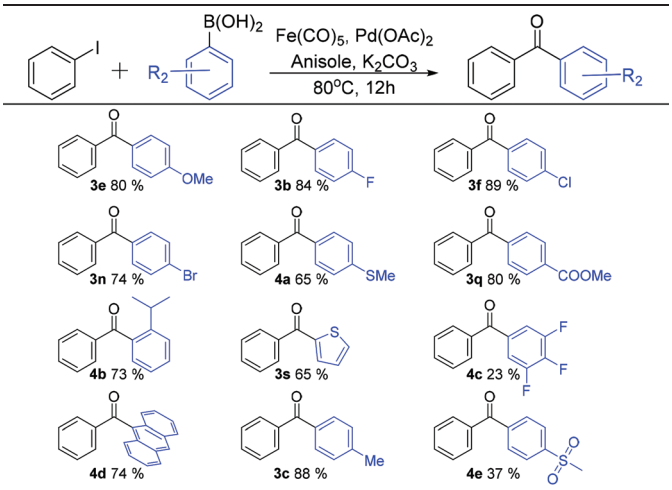

As shown in Table 3, different organoboronic acids were utilised in our new *C*-SMCC methodology. Most of the organoboronic acids underwent carbonylative coupling with good yields. The halogenated aryl iodides were converted into diaryl ketones in very good yields (*e.g.* *p*-F, **3b**, 84%, *p*-Cl, **3f**, 89%, and *p*-Br, **3n**, 74%). Both electron-donating (*p*-Me, **3c**, 88% and *p*-OMe, **3e**, 80%) and electron-withdrawing substituents (*p*-CO_2Me, **3q**, 84%) also gave good yields. The 9-fluorenyl arylboronic acid (**4d**, 74%) was pleasingly formed with a good yield. Notably, thio-moieties were well tolerated. Thus, the biarylketone products bearing *p*-MeS and 2-thiophene were both isolated in 65% yield (**4a** and **3s**). A sterically encumbered substituent, *o*-iPr, gave rise to a 73% yield of **4b**, whilst the organoboronic acids bearing several fluorine atoms or a *p*-SO_2Me group gave lower yields of 23% (**4c**) and 37% (**4e**), respectively.

Encouraged by the results presented above, we subsequently carried out a *C*-SMCC reaction on a gram scale to demonstrate its practical utility. With 5 mmol of **1a**, product **3a** was formed in 86% yield under our optimised conditions (Scheme 1). Furthermore, the phenylenebis–phenylmethanones were synthesized *via* the *C*-SMCC reactions of various diiodobenzenes with phenylboronic acid, in up to 86% yield (Scheme 1, **5a–c**). The results highlight the significant potential of this *C*-SMCC for practical applications.

Finally, we have tested the *C*-SMCC methodology using 4-bromo-anisole and 4-bromo-6-methyl-2-pyrone as exemplar brominated substrates (employing standard conditions as described in Table 2, in the presence and absence of activating DPPF and Xantphos ligands which we hypothesised might assist with C–Br bond activation and CO-migratory insertion steps). However, in the case of 4-bromo-anisole it was left unreacted. For 4-bromo-6-methyl-2-pyrone, a small amount of 4-phenyl-6-methyl-2-pyrone was formed (7%) when the exogenous Xantphos ligand was added (by traditional SMCC reaction).

Green metrics using the CHEM21 toolkit

Clark *et al.* developed a unified metrics toolkit to evaluate the global sustainability of chemical reactions. It was a successful toolkit developed by the CHEM21 consortium consisting of academic and industrial members.[20a] The toolkit is built upon a comprehensive and holistic range of criteria enabling the measurement of how green a reaction is. The toolkit has been applied in the assessment of the synthesis of multicomponent products,[20b] opioid scaffolds,[20c] dialkyl chloramines,[20d] ionic liquids,[20e] solvents,[20f] peptides[20g] and tryptophan C–H bond functionalization chemistry.[20i,h] We recognized that the toolkit would be useful for initial appraisal of the newly developed *C*-SMCC methodology described above. The synthesis of **3a** from 4-iodoacetophenone **1a** and phenylboronic acid **2a** (Scheme 1) was compared with a relevant synthesis involving an activated Pd precatalyst possessing a bis-chelating N-heterocyclic carbene ligand.[21] The literature procedure employed 13.8 bar (200 psi) of CO and 0.01 mol% of Pd pre-catalyst. The methodology from the Chem21 Metrics Toolkit at the first path (key reaction) level was adopted to compare the results, which are collated in Table 4, including the reagent and product stoichiometries.

The data in Table 4 show that the green metrics for the two synthetic methodologies are broadly similar. Surprisingly, this includes atom economy (AE), with our work only being slightly poorer due to one fragment of "$Fe(CO)_2$" not making it into the final product (note: the final destination for Fe is in the form of Fe_2O_3 *vide infra* which is required for Pd catalyst enhancement). However, the AE is dominated by the iodine and boronic acid leaving groups, a necessary and mandatory requirement for the arylation process. More significant however is the Reaction Mass Efficiency (RME) being significantly better for our work. This is because the CO–RM, $Fe(CO)_5$, is an efficient and mild CO source, while the reported reaction conditions employ a 23 molar excess under significant pressure. The same effect can be seen in the Process Mass Intensity (PMI) reaction chemicals. These results are likely more significant, as 3× refills and purges of CO are necessary for the reported[21] pressurised reaction vessel. The inclusion of this practical and necessary requirement gives an RME of 6.7% and a PMI of 14.9. Neither reaction scores well on health and safety, due to the need for liberation of CO (which is formally a necessary requirement for a carbonylation reaction). Lastly, the lower temperature and absence of the need to pressurize give an improved energy demand for our *C*-SMCC methodology.

Table 4 Quantitative and qualitative metrics for the synthesis of **3a** (note: a '$Fe(CO)_2$' fragment is qualitatively a side product from the overall transformation)

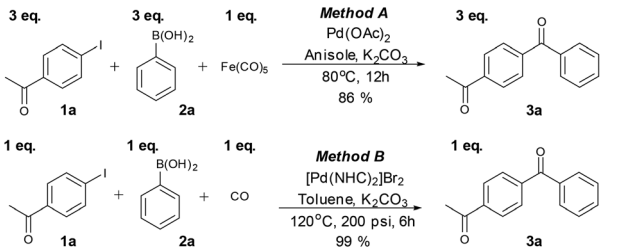

Metric	Method A	Flag	Method B	Flag
Yield	86%		99.0%	
Conversion	94.3%		100%	
Selectivity	91.2%		99%	
Reaction mass efficiency (RME)	23.2%		16.7%	
Atom economy (AE)	39.2%		42.0%	
Solvents	Anisole		Toluene	
Health and safety	H300, H330		H360, H372	
Process mass intensity (PMI)	40.0		25.5	
PMI (reaction chemicals)	4.3		6.0	
PMI (reaction solvents)	35.7		19.5	
Catalyst	Yes		Yes	
Reactor	Batch		Batch	
Elements	B, Pd, I		B, Pd, I	
Energy	80 °C		120 °C	

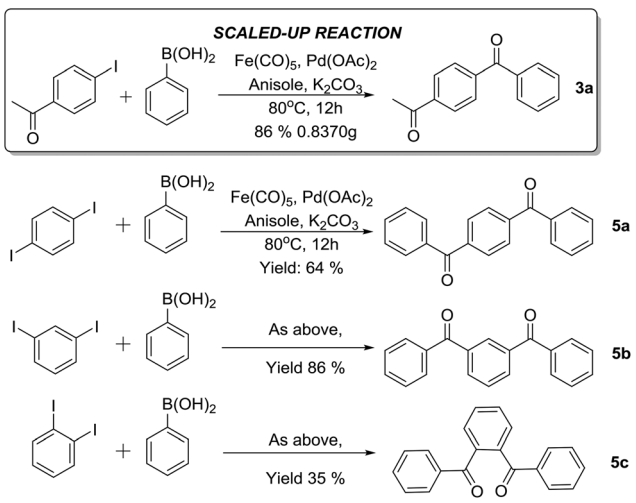

Scheme 1 Examples and gram-scale reaction in practical applications.

Mechanistic studies

To assess further the properties of the metal species formed in the catalytic *C*-SMCC reactions, a series of control experiments were conducted (Scheme 2). Initially, addition of Hg (known to generally suppress surface catalysis) diminished the catalytic activity of the Pd–Fe catalytic system, with neither the carbony-

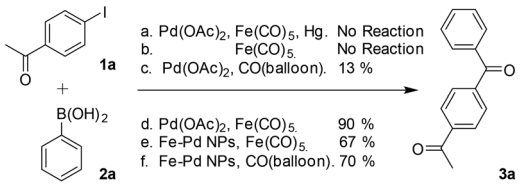

Scheme 2 Control experiments to probe catalyst behaviour.

lative (**3a**) nor non-carbonylative cross-coupling products (**3a′**) detected (Scheme 2a). The Hg poison test supports a heterogeneous/pseudo-heterogeneous Pd-catalysed *C*-SMCC reaction using $Fe(CO)_5$.[22] We succeeded in separating the catalytic Pd–Fe nanoparticle material, which also catalysed a subsequent carbonylative coupling reaction using either additional CORM or CO gas, proceeding with 67% and 70% yields, respectively. Surprisingly, the catalytic Pd–Fe nanoparticles produced the carbonylative product independent of an added CO-source (**3a**, in 15% yield), indicating that CO resides within the Pd–Fe particles, *i.e.* as a CO-reservoir. FT-IR spectroscopic analysis of the fresh isolated metal catalyst material revealed three characteristic CO bands of the particles at 2106, 2029 and 1866 cm^{-1} (Fig. S6, see ESI†), suggesting that the particle surface consists of several carbonyl ligands, *e.g.* η^1-Pd-CO and μ_2-Fe-CO, which derive from the transfer process of CO from CO–RM to ketone products during the Pd-catalysed *C*-SMCC reaction. It is important to note that the *C*-SMCC reaction does not occur without added $Pd(OAc)_2$ (Scheme 2b). Starting from $Pd(OAc)_2$, the Pd-catalysed *C*-SMCC reaction with CO gas was found to afford only a 13% yield of biaryl ketone **3a** (Scheme 2c), indicating again that $Fe(CO)_5$ not only acted as a CO–RM, but also enhanced Pd-catalyst performance.

To further characterize the catalytically active Pd–Fe particles, Transmission Electron Microscopy (TEM) measurements were conducted. The experiments showed the presence of 2 nm sized Pd–Fe nanoparticles over a large area (histogram inset in Fig. 2a). Lattice fringes were observed in the high-resolution TEM images (Fig. 2b), showing that the inter-planar distances approximate to 0.226 nm and 0.198 nm, corresponding to the (200) and (111) planes of the Pd metal. The assignment was confirmed using Fast Fourier Transform (FFT) and inverse FFT images (inset in Fig. 2b).

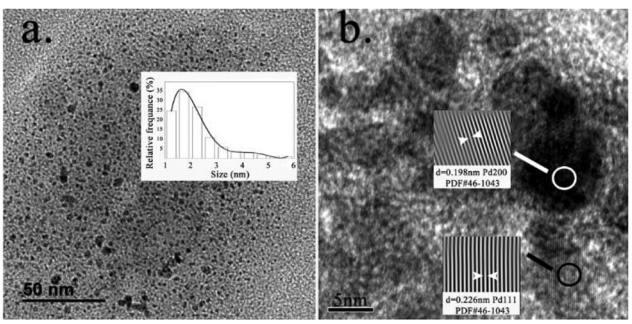

Fig. 2 (a) HRTEM images of size distribution and (b) lattice fringes.

The chemical state of the Pd–Fe nanoparticle surface was analysed by XPS (Fig. 3 and ESI S3†). Fig. 3 shows the XPS core level spectra for Pd 3d and Fe 2p, characterized by spin–orbit splitting (Pd $3d_{5/2}$, $3d_{3/2}$ and Fe $2p_{3/2}$, $2p_{1/2}$ components), where the peaks at 335.6 and 340.8 eV result from Pd $3d_{5/2}$ and Pd $3d_{3/2}$, respectively. The Pd species are characterised as being in an oxidation state of zero. Fe^{III} was confirmed based on the peaks at 710.6 and 724.1 eV, corresponding to Fe $2p_{3/2}$ and Fe $2p_{1/2}$, respectively. The side peaks were attributed to the oxide; thus Fe exists in the form of Fe_2O_3. The EDAX mapping analysis confirmed the composition of the Pd–Fe nanoparticles deriving from Fe, Pd and O, which is fully consistent with our deduction (ESI S4†). SEM images show the morphology of the Pd–Fe nanoparticles (Fig. S5, see the ESI†).

Finally, the recyclability of the Pd–Fe nanoparticles was assessed. The Pd–Fe nanoparticles were first isolated from a reaction of **1a** + **2a** → **3a**, by filtration, and then sequentially washed with water and ethyl acetate. The *C*-SMCC reaction **1a** + **2a** → **3a** was then recharged with fresh $Fe(CO)_5$ and the isolated catalyst. At each cycle we found that the isolated catalyst can be recycled giving **3a**, with the yields of **3a** going from 90 to 50% over the 4 cycles. The deactivation of the heterogeneous Pd–Fe nanocatalyst species can be attributed to an excess Fe residue being deposited onto the heterometallic surface, either blocking the catalytically active sites or causing a restructuring of the catalyst surface (Fig. 4A).[15,21] Interestingly, in the absence of $Fe(CO)_5$, the isolated Pd–Fe nanoparticles also independently catalyzed the efficient SMCC reaction of **1a** + **2a** → **3a′** (Fig. 4B). A small amount of carbonylative product **3a** is formed in the first cycle, formed from residual CO from the Pd–Fe nanoparticle catalyst. Crucially,

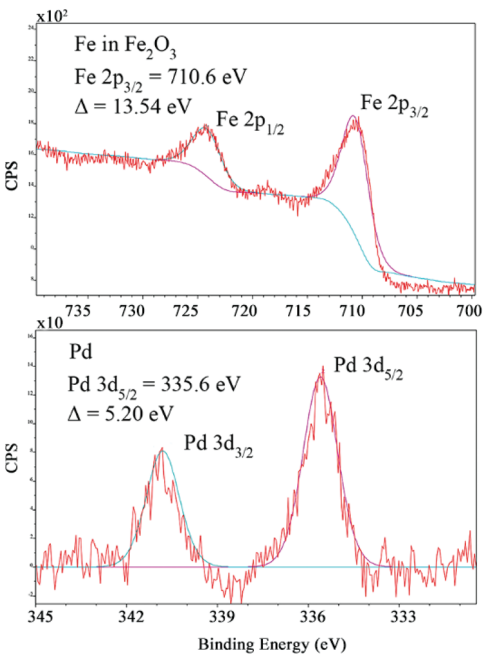

Fig. 3 XPS images of the Pd–Fe catalyst nanoparticle material, with Fe_2O_3 and Pd^0 prominent species.

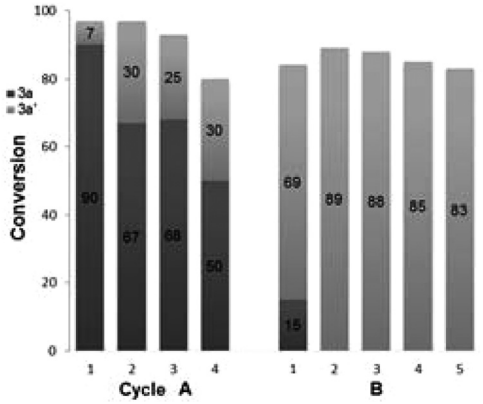

Fig. 4 Recyclability of the Suzuki–Miyaura carbonylative cross-coupling (cycle A) and feasibility of the Pd–Fe nanoparticle catalyst in the SMCC reaction of iodobenzene and phenylboronic acid to give benzophenone (cycle B).

the yield of **3a′** was over 80% for the subsequent cycles (2–5). These results are in accordance with the unique cooperative activity of a Pd–Fe bimetallic catalytic system reported by Lipshutz *et al.* for standard SMCC reactions (Fig. 4B).[17]

Conclusions

In conclusion, we have developed a highly efficient synthetic strategy for accessing biaryl ketones *via* CO-gas free carbonylative Suzuki–Miyaura cross-couplings, using anisole as a green solvent.[23] The green credentials of the methodology were compared with those of a recently reported reaction employing a novel and highly active Pd precatalyst possessing a bis-chelating carbene ligand. The Fe–Pd nanoparticles generated *in situ* from mixing '$Pd(OAc)_2$' and $Fe(CO)_5$ are the key factor in the high catalytic efficiency observed in our study. The structural features of the *in situ* Fe–Pd nanoparticles were evaluated by TEM, EDAX, XPS, SEM and FT-IR spectroscopy, demonstrating the narrow size distribution, averaged ~2 nm, which is the so-called 'Goldilocks size' for effective cross-coupling catalysis under reducing conditions.[24] We believe that the particles consist primarily of Fe_2O_3 and the Pd metal, possessing a relaxed porous surface. Based on the above structural information, the efficacy of the *C*-SMCCs can be reasonably attributed to the synergistic effect of bimetallic Pd–Fe NPs, demonstrating the superiority over monometallic catalysis, which ought to facilitate further applications in catalysis, materials science, and organic synthesis. Studies directed toward understanding metal–metal interactions and cooperativity, particularly in bimetallic NPs,[25] and their applications, are currently underway.

Conflicts of interest

There are no conflicts to declare.

Acknowledgements

This work was supported by the grant from the National Natural Science Foundation of China (21371112 and 21446014), the 111 Project (B14041), the Fundamental Funds Research for the Central Universities (No. GK201501005, GK201503029, and 2016CSY002), the grant from the Fundamental Doctoral Fund of Ministry of Education of China (20120202120005), and the Program for Changjiang Scholars and Innovative Research Team in University (IRT_14R33). I. J. S. F. is grateful to the Royal Society for University Research Fellowship (2004-12). We thank Syngenta and the University of York for the iCASE funding and studentship to T. J. B. We also acknowledge the Leverhulme Trust for funding, enabling us to initiate this research (W. Z., I. J. S. F., and J. M. L.).

Notes and references

1 T. Ishiyama, H. Kizaki, N. Miyaura and A. Suzuki, *Tetrahedron Lett.*, 1993, **34**, 7595.
2 Y. Zhong and W. Han, *Chem. Commun.*, 2014, **50**, 3874.
3 D. G. Hall, *Boronic Acids-Preparation and Applications in Organic Synthesis, Medicine and Materials*, Wiley-VCH, Weinheim, 2011, vol. 2.
4 (*a*) K. Maeyama, K. Yamashita, H. Saito, S. Aikawa and Y. Yoshida, *Polym. J.*, 2012, **44**, 315; (*b*) W. Sharmoukh, K. C. Ko, C. Noh, J. Y. Lee and S. U. Son, *J. Org. Chem.*, 2010, **75**, 6708; (*c*) F. Boscá and A. Miranda, *J. Photochem. Photobiol., B*, 1998, **43**, 1; (*d*) G. Dormán and G. D. Prestwich, *Biochemisty*, 1994, **33**, 5661; (*e*) S. Budavari, *The Merck Index*, Merck, Rahway, USA, 11th edn, 1989.
5 For some recent reviews on Pd-catalyzed carbonylation, see: (*a*) X.-F. Wu, H. Neumann and M. Beller, *Chem. Rev.*, 2013, **113**, 1; (*b*) X.-F. Wu, H. Neumann and M. Beller, *Chem. Soc. Rev.*, 2011, **40**, 4986; (*c*) R. Grigg and S. P. Mutton, *Tetrahedron*, 2010, **66**, 5515; (*d*) A. Brennführer, H. Neumann and M. Beller, *Angew. Chem., Int. Ed.*, 2009, **48**, 4114; (*e*) M. Beller and X.-F. Wu, *Transition Metal Catalyzed Carbonylation Reactions*, Springer-Verlag, Berlin Heidelberg, 2013; (*f*) Z.-L. Zhu, W.-Q. Zhang and Z.-W. Gao, *Prog. Chem.*, 2016, **28**(11), 1616.
6 A. Petz, G. Péczely, Z. Pintér and L. Kollár, *J. Mol. Catal. A: Chem.*, 2006, **255**, 97.
7 F. Jin and W. Han, *Chem. Commun.*, 2015, **51**, 9133.
8 I. J. S. Fairlamb, S. Grant, P. McCormack and J. Whittall, *Dalton Trans.*, 2007, **8**, 859.
9 T. Morimoto and K. Kakiuchi, *Angew. Chem., Int. Ed.*, 2004, **43**, 5580.
10 (*a*) S. D. Friis, A. T. Lindhardt and T. Skrydstrup, *Acc. Chem. Res.*, 2016, **49**(4), 594; (*b*) P. Hermange, A. T. Lindhardt, R. H. Taaning, K. Bjerglund, D. Lupp and T. Skrydstrup, *J. Am. Chem. Soc.*, 2011, **133**, 6061; (*c*) A. Ahlburg, A. T. Lindhardt, R. H. Taaning, A. E. Modvig and T. Skrydstrup, *J. Org. Chem.*, 2013, **78**, 10310.

11 P. Gautam and B. M. Bhanage, *Catal. Sci. Technol.*, 2015, **5**, 4663.
12 For the recent progress in CORMs, see: (*a*) S. García-Gallego and G. J. L. Bernardes, *Angew. Chem., Int. Ed.*, 2014, **53**, 9712; (*b*) U. Schatzschneider, *Br. J. Pharmacol.*, 2014, **172**, 1638.
13 (*a*) E. J. Corey and L. S. Hegedus, *J. Am. Chem. Soc.*, 1969, **91**, 1233; (*b*) E. Yoshisato, M. Ryang and S. Tsutsumi, *J. Org. Chem.*, 1968, **34**, 1500.
14 (*a*) N.-F. K. Kaiser, A. Hallberg and M. Larhed, *J. Comb. Chem.*, 2002, **4**, 109; (*b*) J. Wannbeg and M. Larhed, *J. Org. Chem.*, 2003, **68**, 5750.
15 (*a*) S. R. Borhade, A. Sandström and P. I. Arvidsson, *Org. Lett.*, 2013, **15**, 1056; (*b*) F. Jafarpour, P. Rashidi-Ranjbar and A. O. Kashani, *Eur. J. Org. Chem.*, 2011, 2128; (*c*) W. J. Ang, L.-C. Lo and Y. Lam, *Tetrahedron*, 2014, **70**, 8545.
16 (*a*) T. Vlaar, E. Ruijter, B. U. W. Maes and R. V. A. Orru, *Angew. Chem., Int. Ed.*, 2013, **52**, 7084; (*b*) J. W. Collet, T. R. Roose, E. Ruijter, B. U. W. Maes and R. V. A. Orru, *Angew. Chem., Int. Ed.*, 2020, **59**, 540.
17 S. Handa, Y. Wang, F. Gallou and B. H. Lipshutz, *Science*, 2015, **349**, 1087.
18 M. Alami, C. Amatore, S. Bensalem, A. Choukchou-Brahim and A. Jutand, *Eur. J. Inorg. Chem.*, 2001, **2001**, 2675.
19 (*a*) L. Kumar, S. K. Dhawan, M. N. Kamalasanan and S. Chandra, *Thin Solid Films*, 2003, **441**, 243; (*b*) A. Banerjee, A. Sahana, S. Das, S. Lohar, B. Sarkar, S. K. Mukhopadhyay, J. S. Matalobos and D. Das, *Dalton Trans.*, 2013, **42**, 16387; (*c*) Y. Niko, Y. Hiroshige, S. Kawauchi and G. Konishi, *J. Org. Chem.*, 2012, **77**, 3986; (*d*) Z. Zhu, E. Shao, S. Xu, H. Sun, G. Zhang, Z. Xie, W. Zhang and Z. Gao, *RSC Adv.*, 2016, **6**, 76883.
20 (*a*) C. R. McElroy, A. Constantinou, L. C. Jones, L. Summerton and J. H. Clark, *Green Chem.*, 2015, **17**, 3111; (*b*) S. Abou-Shehada, P. Mampuys, B. U. W. Maes, J. H. Clark and L. Summerton, *Green Chem.*, 2017, **19**, 249; (*c*) N. McStay, Z. Molphy, A. Coughlan, A. Cafolla, V. McKee, N. Gathergood and A. Kellett, *Nucleic Acids Res.*, 2017, **45**, 527; (*d*) A. J. Blacker and K. E. Jolley, *Beilstein J. Org. Chem.*, 2015, **11**, 2408; (*e*) A. Jordan, A. Haiß, M. Spulak, Y. Karpichev, K. Kümmerer and N. Gathergood, *Green Chem.*, 2016, **18**, 4374; (*f*) S. Jin, F. Byrne, C. R. McElroy, J. Sherwood, J. H. Clark and A. J. Hunt, *Faraday Discuss.*, 2017, **202**, 157; (*g*) K. E. Jolley, W. Nye, C. G. Niño, N. Kapur, A. Rabion, K. Rossen and A. J. Blacker, *Org. Process Res. Dev.*, 2017, **21**, 1557; (*h*) A. J. Reay, L. A. Hammarback, J. T. W. Bray, T. Sheridan, D. Turnbull, A. C. Whitwood and I. J. S. Fairlamb, *ACS Catal.*, 2017, **7**, 5174; (*i*) A. J. Reay, T. J. Williams and I. J. S. Fairlamb, *Org. Biomol. Chem.*, 2015, **13**, 8298.
21 W. Mansour, M. Fettouhi and B. E. Ali, *Appl. Organomet. Chem.*, 2020, **34**, e5636.
22 T. Storr, A. Firth, K. Wilson, K. Darley, C. Baumann and I. J. S. Fairlamb, *Tetrahedron*, 2008, **64**, 6125.
23 We note that anisole, as a green solvent, has an excellent sustainability ranking, particularly in hydroformylation, see: F. G. Delolo, E. N. dos Santos and E. V. Gusevskaya, *Green Chem.*, 2019, **21**, 1091.
24 A. J. Reay and I. J. S. Fairlamb, *Chem. Commun.*, 2015, **51**, 16289.
25 For lead references, see: K. Mishra, N. Basavegowdaa and Y. R. Lee, *Catal. Sci. Technol.*, 2015, **5**, 2612.

